

# SSSP Homework #2

Matteo Pettenò - Student ID: 10868930

## 1 WDF Crossover

### 1.1 Schemes

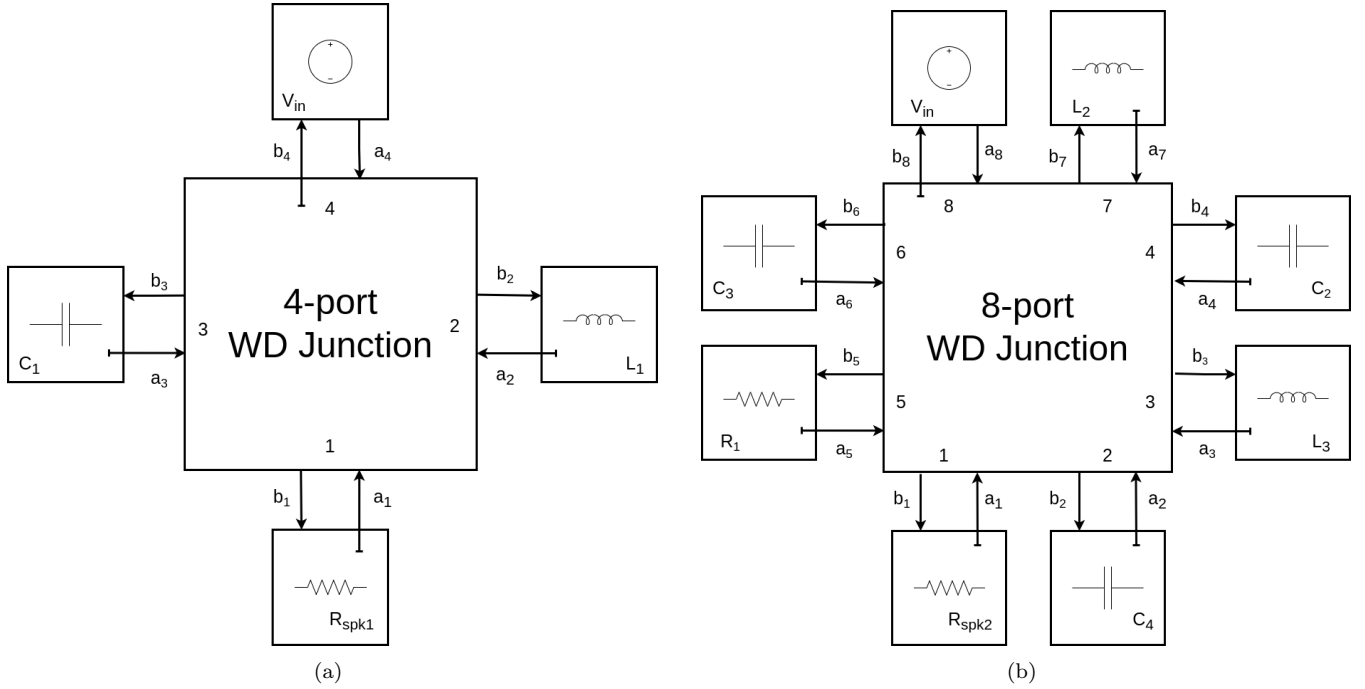


Figure 1: (a) HPF 4-port WD Junction (b) BPF 8-port WD Junction

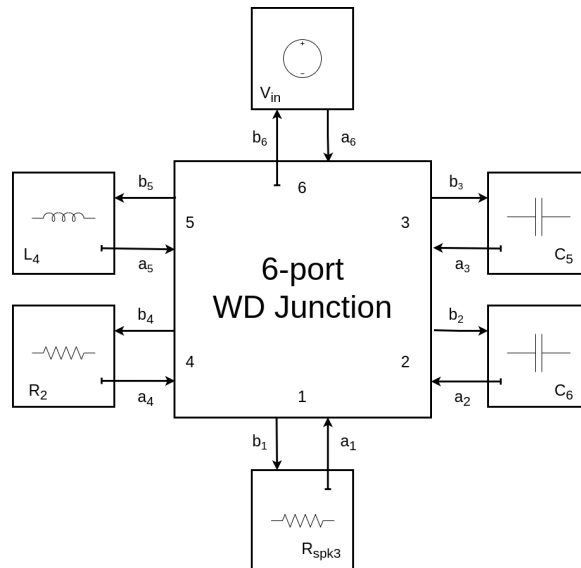


Figure 2: LPF 6-port WD Junction

## 1.2 Description

The given crossover's reference circuit has been represented as a WDF structure using only three N-port topological junctions, one per subcircuit (Fig. 1 and Fig. 2). Below we intend to briefly explain how the scattering matrix was derived only for BPF's 8-port WD junction, knowing that the procedure was identical for LPF and HPF.

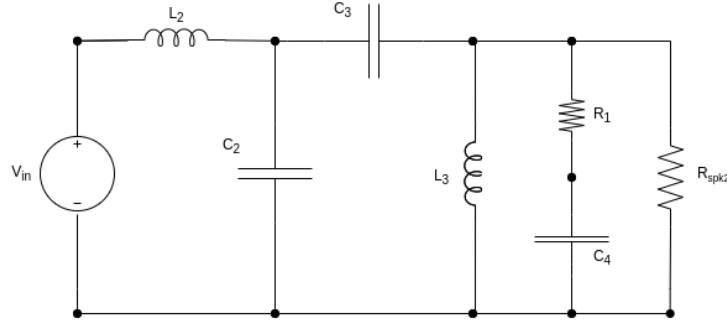


Figure 3: BPF Subcircuit

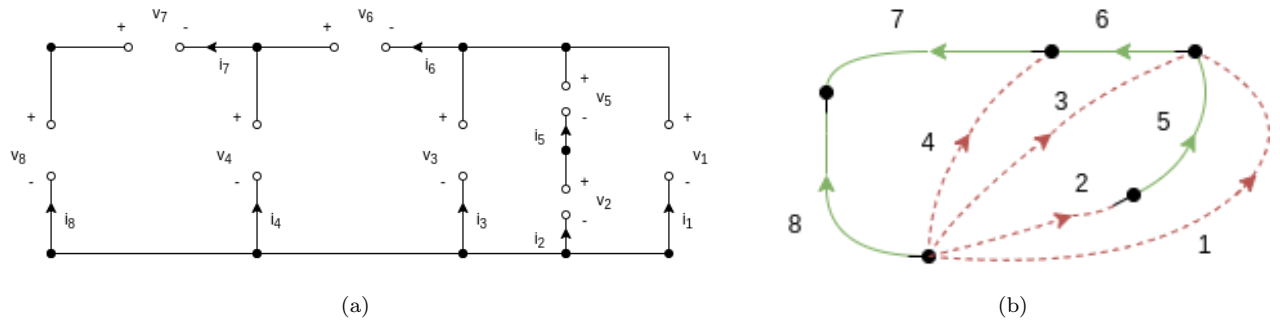


Figure 4: (a) BPF Port Circuit (b) BPF Digraph

In order to find a subset of independent port voltages/port currents, starting from the subcircuit for the BPF (Fig. 3), we first derived its topological connection network (Fig. 4a) and then its digraph (Fig. 4b) with one possible tree-cotree decomposition: the ports that belong to the tree are shown in green, while the red ones belong to the cotree.

$$\mathcal{T} = \{5, 6, 7, 8\} \quad \mathcal{C} = \{1, 2, 3, 4\}$$

We note that both the tree and the cotree contain the same number of ports and this means that for the circuit the number of independent port voltages is equal to the number of independent port currents (this also occurs for the other two subcircuits). So from a computational point of view it is the same to choose one or the other path. By choosing to apply KLC we obtain the following system of equations for currents:

$$\begin{cases} i_5 = i_2 \\ i_6 = i_1 + i_3 + i_5 \\ i_7 = -i_8 \\ i_8 = -(i_1 + i_2 + i_3 + i_4) \end{cases} \Rightarrow \begin{cases} i_5 = i_2 \\ i_6 = i_1 + i_2 + i_3 \\ i_7 = i_1 + i_2 + i_3 + i_4 \\ i_8 = -(i_1 + i_2 + i_3 + i_4) \end{cases} \quad (1)$$

And we obtain the *fundamental loop matrix*:

$$i = B^T i_l \Rightarrow \begin{bmatrix} i_1 \\ i_2 \\ i_3 \\ i_4 \\ i_5 \\ i_6 \\ i_7 \\ i_8 \end{bmatrix} = \begin{bmatrix} 1 & 0 & 0 & 0 \\ 0 & 1 & 0 & 0 \\ 0 & 0 & 1 & 0 \\ 0 & 0 & 0 & 1 \\ 0 & 1 & 0 & 0 \\ 1 & 1 & 1 & 0 \\ 1 & 1 & 1 & 1 \\ -1 & -1 & -1 & -1 \end{bmatrix} \begin{bmatrix} i_1 \\ i_2 \\ i_3 \\ i_4 \end{bmatrix} \quad (2)$$

### 1.3 Free parameters

The free parameters for each WDF scheme can be set as follow:

- **HPF**

- $Z_1 = R_{spk1}$
- $Z_2 = (2 \cdot L_1)/T_s$
- $Z_3 = T_s/(2 \cdot C_1)$

- **LPF**

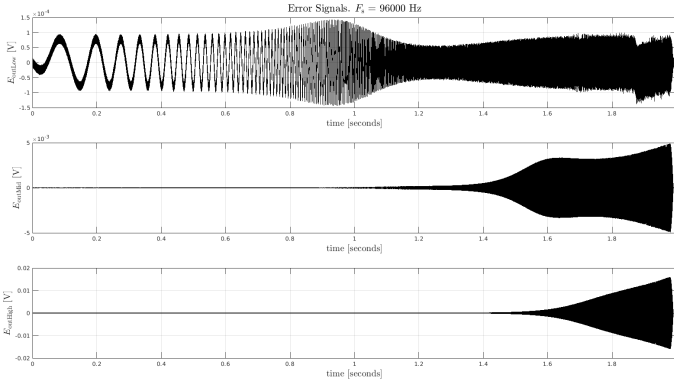
- $Z_1 = R_{spk3}$
- $Z_2 = T_s/(2 \cdot C_6)$
- $Z_3 = T_s/(2 \cdot C_5)$
- $Z_4 = R_2$
- $Z_5 = (2 \cdot L_4)/T_s$

- **BPF**

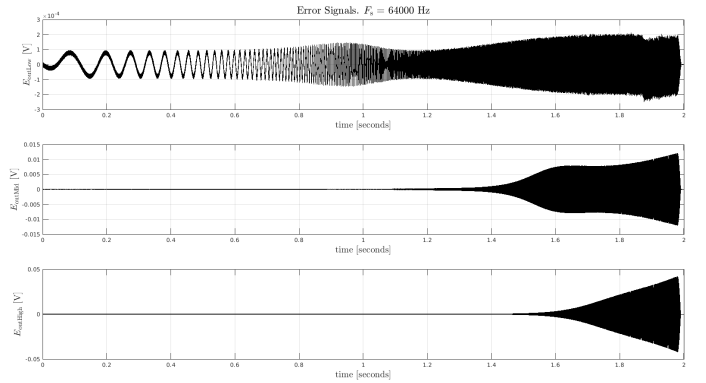
- $Z_1 = R_{spk2}$
- $Z_2 = T_s/(2 \cdot C_4)$
- $Z_3 = (2 \cdot L_3)/T_s$
- $Z_4 = T_s/(2 \cdot C_2)$
- $Z_5 = R_1$ ;
- $Z_6 = T_s/(2 \cdot C_3)$
- $Z_7 = (2 \cdot L_2)/T_s$

Free parameters  $Z_4$ ,  $Z_8$ ,  $Z_6$  respectively for HPF, BPF and LPF, are set by computing the scattering matrix  $S$  and then solving  $s_{nn} = 0$  as suggested in the assignment.

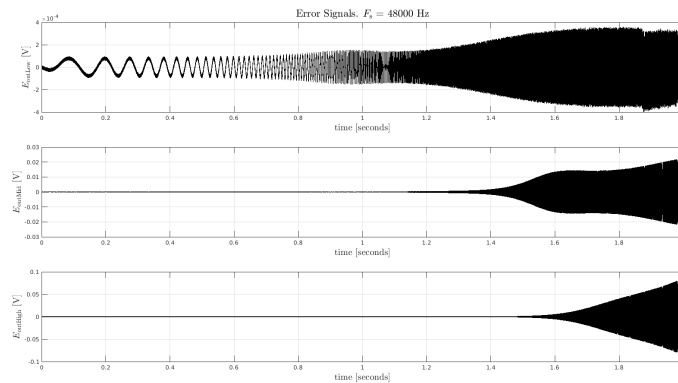
### 1.4 Error signals plots



(a)



(b)



(c)

Figure 5: (a) 96 KHz Error Signals (b) 64 KHz Error Signals (c) 48 KHz Error Signals

## 2 Questions

### 2.1 Question 1

Observing the graphs of the error we notice that in terms of amplitude peaks the error is greater for the output of the high pass filter and decreases by about an order of magnitude the more we move towards the low frequencies. So we can say that the high pass filter WDF output signals is the least accurate one. This is due to the fact that we are using the *Bilinear Transform* for the discrete-time frequency approximation:

$$s \leftarrow \frac{2}{T_s} \frac{1 - z^{-1}}{1 + z^{-1}} \implies jw \leftarrow \frac{2}{T_s} \frac{e^{j\tilde{w}T_s} - 1}{e^{j\tilde{w}T_s} + 1} \implies jw \leftarrow j \frac{2}{T_s} \tan\left(\tilde{w} \frac{T_s}{2}\right) \quad (3)$$

The last relation in Eq. 3 shows us that the continuous-time frequency  $w$  can be expressed in closed-form as a function of the discrete-time frequency  $\tilde{w}$  with the *warping mapping*:

$$w = \frac{2}{T_s} \tan\left(\tilde{w} \frac{T_s}{2}\right) \quad (4)$$

From 4 we see that if  $\tilde{w} \rightarrow 0$  then we are in the linear region of the tangent that can then be approximated with the value of its argument leading us to an accurate mapping between discrete and continuous domain frequencies.

$$\tilde{w} \rightarrow 0 \implies \tan\left(\tilde{w} \frac{T_s}{2}\right) = \tilde{w} \frac{T_s}{2} \implies w = \tilde{w} \quad (5)$$

Conversely, as we move towards the high frequencies, the tangent begins to have its effect and the two frequencies will be much more different.

### 2.2 Question 2

By increasing the sampling frequency the error decreases for all the three WDF output signals (obviously the difference between the three frequency bands remains, as explained in the previous question). This is an expected behavior since increasing the sampling frequency also means increasing the Nyquist frequency and therefore extending the useful low frequency range in which we have seen that the *Bilinear Transform* works better.

### 2.3 Question 3

In wave digital domain we are able to find an explicit computational scheme such that no iterative solver are required only if we have a reference analog network with at most one non-linear element. If we add a single diode in parallel with the twitter resistor  $R_H$  we end up with two non-linear elements in the circuit and thus we can't use the tree computational scheme anymore but we have to use multivariate iterative solvers, such as Newton-Raphson solvers. But if we replace the ideal voltage source with the resistive one, the only non-linear element in the circuit is the diode so we can use again the tree computational scheme where the diode becomes the root with its scattering relation given by:

$$b[k] = a[k] + 2Z[k]I_s - 2\eta V_{th}W\left(\frac{Z[k]I_s}{\eta V_{th}}e^{\frac{Z[k]I_s + a[k]}{\eta V_{th}}}\right) \quad (6)$$

### 2.4 Question 4

The constitutive equations of an inductor in the continuous-time domain and in the Laplace domain are:

$$v(t) = L \cdot \frac{di(t)}{dt} \xrightarrow{\mathcal{L}} V(s) = sL \cdot I(s) \quad (7)$$

Now if we consider the *Backward Euler Method* transform and we apply it to Eq. 7, we have:

$$s \leftarrow \frac{1 - z^{-1}}{T_s} \implies V(z) = \frac{1 - z^{-1}}{T_s} L \cdot I(z) \implies V(z) = \frac{L}{T_s} \cdot I(z) - \frac{L}{T_s} z^{-1} \cdot I(z) \quad (8)$$

And we obtain the discrete-time approximation of 7 by applying the inverse  $\mathcal{Z}$  transform in 8:

$$v[k] = \frac{L}{T_s} \cdot i[k] - \frac{L}{T_s} \cdot i[k-1] \quad (9)$$

The general one-port linear elements constitutive equation and its generic scattering relation in WDF domain are given by:

$$v[k] = R_e[k] \cdot i[k] + V_e[k] \quad (10)$$

$$b[k] = \frac{R_e[k] - Z[k]}{R_e[k] + Z[k]} \cdot a[k] + \frac{2Z[k]}{R_e[k] + Z[k]} \cdot V_e[k] \quad (11)$$

and by comparing 9 with 10 we note that:

$$R_e[k] = \frac{L}{T_s}, \quad V_e[k] = -\frac{L}{T_s} \cdot i[k-1], \quad (12)$$

12 applied to 11 gives us the corresponding (non-adapted) scattering relation in the WD domain for the inductor. In order to get rid of the instantaneous dependency between  $b[k]$  and  $a[k]$  in Eq. 11 and thus adapt the scattering relation, we need to set the free parameter equals to the resistive parameter which leads us to the following adaptation condition:

$$Z[k] = R_e[k] = \frac{L}{T_s} \quad (13)$$

And with this condition the adapted scattering relation becomes:

$$b[k] = V_e[k] = -\frac{L}{T_s} \cdot i[k-1], \quad (14)$$

The inverse mapping between Wave and Kirchoff variables is:

$$i[k-1] = \frac{a[k-1] - b[k-1]}{2Z[k-1]} = \frac{a[k-1] - b[k-1]}{2R_e[k-1]} = \frac{a[k-1] - b[k-1]}{2\frac{L}{T_s}} \quad (15)$$

by applying 15 in 14 we finally get the wave mapping relation in case of adaptation:

$$b[k] = \frac{b[k-1] - a[k-1]}{2} \quad (16)$$

The table below resumes the WD model for the inductor using the *Backward Euler Method*:

Constitutive Eq.	Wave Mapping in Case of Adaptation	Adaptation Condition
$v(t) = L \cdot \frac{di(t)}{dt}$	$b[k] = \frac{b[k-1] - a[k-1]}{2}$	$Z[k] = \frac{L}{T_s}$

Table 1: WD Inductor Model based on Backward Euler Method.